

## METALLICITY AND AGE OF DISC STARS

Misha Haywood

Observatoire de Paris, GEPI / CNRS UMR 8111, 92195 Meudon cedex, France

### ABSTRACT

Disc stars will represent the vast majority of objects in the Gaia Catalogue. For several tens of millions of F and G type stars, parallaxes and multi-colour photometry will permit the determination of age and metallicity to good accuracy. I illustrate the present level of our knowledge on ages and metallicities of disc stars in the solar neighbourhood, and discuss their properties from available data. Looking in retrospect to what has been achieved with Hipparcos data on field stars, we know that an important source of uncertainty in the determination of ages are the atmospheric parameters. I show how systematic biases on these parameters affect the determination of evolutionary patterns such as the age-metallicity distribution, and look for possible implications for Gaia.

Key words: Metallicity; Age; Galactic Disc.

### 1. INTRODUCTION

Disc stars will represent the majority of the content of the Gaia Catalogue, with no less than several hundreds of millions of objects. Assuming the kind of material that is foreseen with Gaia, ages will be determined up to several kpc with an accuracy barely achieved within 100pc with Hipparcos parallaxes. What should we expect from this kind of accuracy? Looking at the literature since the publication of the Hipparcos Catalogue (ESA 1997), no compelling evidence of an age-metallicity relation (hereafter AMR) or bursts in the star formation history (hereafter SFH) has emerged. It may be that a correlation between age and metallicity doesn't exist, or has been smeared by radial diffusion in the galactic disc; it may also be that the disc has endured no significant burst. However, we show below that if these features exist, they are unlikely to have been found, given our present level of accuracy in age determination. The main reason is that atmospheric parameters are not determined, for statistically significant samples (few thousands of objects), with a level of accuracy sufficient to get the best out of the parallaxes. This limitation has been known for some time, and it is one of the reasons Gaia has also been conceived as a photometric and spectroscopic mission. In principle, Gaia can achieve much better results for age determinations

for several reasons. The first one is that for a substantial number of objects, parallaxes will be determined to better than 1% relative accuracy, which, with the measurements of numerous stellar masses and complementary data obtained from the ground (angular diameters, spectra, infrared data) or from other satellites before Gaia (asteroseismology), will allow extensive calibration of stellar models over all the HR diagram, at all metallicities. The second reason is that Gaia will provide highly homogeneous and accurate photometric data. When working on statistically significant samples taken from the Hipparcos Catalogue, it must be noted that this is one of the main sources of uncertainty for determining ages of the stars.

We discuss the present level of uncertainties on the atmospheric parameters  $T_{\text{eff}}$  and  $[\text{Fe}/\text{H}]$ . Then, we present a general picture of the metallicity distribution of A to K stars in the solar neighbourhood, discussing the evidences of an AMR *prior* to age determination. We design a simple test to check our ability to recover the AMR or SFH, assuming different bias and random uncertainties on atmospheric parameters  $M_v$ ,  $T_{\text{eff}}$  and  $[\text{Fe}/\text{H}]$ .

### 2. AGE TRENDS AND UNCERTAINTIES: PRESENT STATUS

We briefly review evidences (or the lack of) of age trends in the solar neighbourhood, as reflected in the AMR and SFH. The most precise method to estimate the age of a star is the fit of an isochrone to the position of a star in the HR diagram, implying that we have an estimate of its absolute magnitude, effective temperature and metallicity. In the solar neighbourhood, the accuracy of the first parameter is given by the Hipparcos parallaxes. The two others are determined by a variety of methods and data that are subject to large uncertainties, either random or systematic which are discussed below.

#### 2.1. Ages Trends: the AMR and SFH

The question of an AMR in the galactic disc was addressed at least since the seventies, with the problematic (King 1971) existence of old, metal-rich objects in this context being discussed simultaneously. The first study clearly suggesting such relation is that of Powell (1972),

while more recent work (Edvardsson et al. 1993) have cast some doubt on its reality. Since the publication of the Hipparcos Catalogue, several studies have pointed to a large dispersion and no trend with age (Feltzing et al. 2001; Ibukiyama & Arimoto 2002), while a study based on chromospheric activity by Rocha-Pinto et al. (2000b) found a rather tight relation. More recently, Nordström et al. (2004) found results similar to that of Feltzing et al. (2001), (using essentially the same data and calibrations), while Pont & Eyer (2004), focusing on a restricted but cleaner sample point to a possible correlation.

The results on the SFH are just as uncertain as for the AMR. The published papers can broadly be classified in two groups: studies which measure a trend in the star formation activity with age, and those which claim to have found bursts of star formation. In principle, this would be only a matter of resolution in age. However, studies based on similar kind of data often differ in their conclusions. For instance, Barry (1988) and Soderblom et al. (1991), using chromospheric activity, find a depression at 1–3 Gyrs, while Rocha-Pinto et al. (2000a) find a burst at 2–3 Gyrs. Rocha-Pinto et al. (2000a) find a depression in star formation activity between 1 and 2 Gyrs, while Hernandez et al. (2000) find an increasingly high star formation activity in this same range. Using the Hipparcos HR diagram (but to metallicity estimates), Bertelli & Nasi (2001) find an increasing SFR ( $\times 2.5$ ), together with Vergely et al. (2002) ( $\times 6$ ). However, given that Bertelli & Nasi (2001) don't take into account scale height increase with ages, their result rather points to a constant SFH.

## 2.2. Uncertainties in Atmospheric Parameters

Current random errors on the determination of effective temperature and metallicity from colour indices on large samples of F and G disc stars are of the order of 150 K and 0.15 dex (better accuracy can be obtained on individual object or small samples). Systematic uncertainties of the same order affect these two parameters, as is described below. For local samples (within 100 pc), which benefit from the Hipparcos parallaxes, the main source of uncertainty in age determination is not parallax, but effective temperature and metallicity.

### 2.2.1. Effective temperatures

In Figure 1, we compare 4 different scales, giving  $T_{\text{eff}}$  as a function of  $B-V$  at solar metallicity and based on different effective temperature estimators (spectroscopic, infrared flux method, indirect ( $V-K$ ,  $T_{\text{eff}}$ ) scale). We use the scale of Gratton et al. (1996) as a reference to which we compare the others. As can be seen on the plot, there are differences amounting to 100–300 K, depending on colour, the most important disagreement being between the scale of Gratton et al. (1996) and the others.

In view of the high dispersion, it is difficult to choose between the different scales, and we need an external estimator of the effective temperature. This is given by the

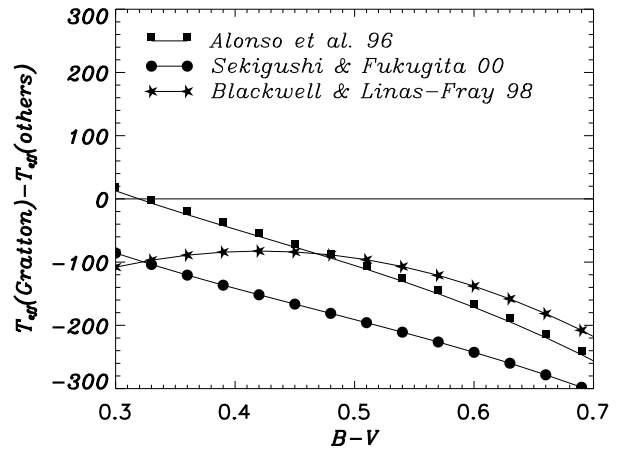


Figure 1. Difference between the effective temperature determine using 4  $T_{\text{eff}}$ -colour calibrations, at solar metallicity. The calibration of Gratton et al. (1996) is used as a reference.

Stefan-Boltzmann relation, and the most recent measurements of apparent angular diameters. For a few nearby dwarfs, it has become possible to measure apparent stellar diameters from interferometry. Although these measurements are still sparse, they are sufficient to establish a fundamental scale to which we can compare available calibrations of temperature as a function of colour.

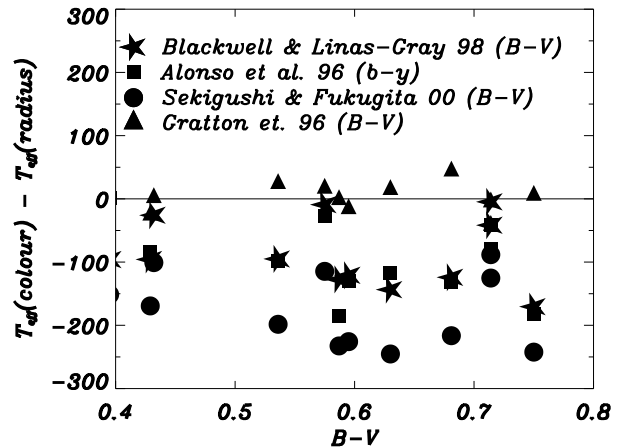


Figure 2. Difference between the effective temperature determine from  $B-V$  or  $b-y$  index, with the effective temperature from recent angular diameter measurements of dwarfs and bolometric luminosity, through the Stefan-Boltzmann relation.

For several stars for which angular diameters have been recently published, we have computed  $T_{\text{eff}}$  through the Stefan-Boltzmann relation, and compare it with the one given by other calibrations. The differences are given in Figure 2, showing again a dispersion between calibrations of the order of 100 to 200K, and a general systematic underestimate of about 150K, except that of Gratton et al. which shows good agreement with  $T_{\text{eff}}$  from angular diameters.

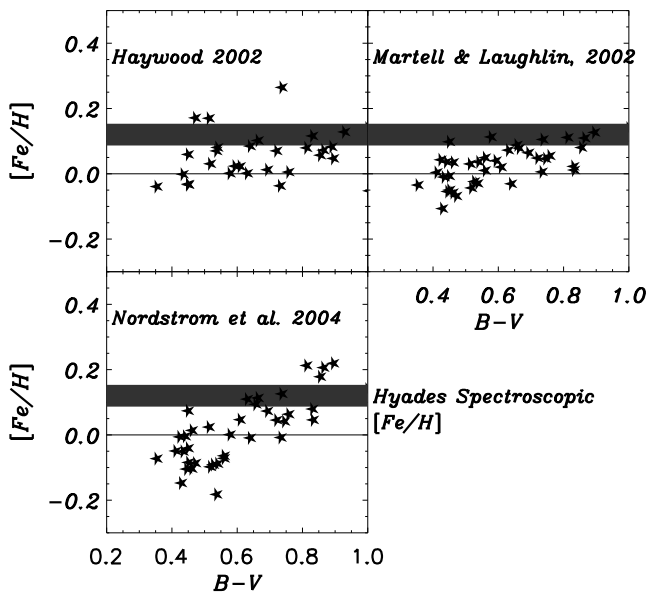


Figure 3. Application of metallicity calibrations of Strömgren photometry to the Hyades stars. All calibrations underestimate the spectroscopic metallicity (in the range 0.10–0.15 dex) by 0.1 to 0.3 dex, depending on colour. The most severe underestimates is for F stars.

### 2.2.2. Metallicities

The largest photometric data base for determining metallicities of solar neighbourhood stars is that of Strömgren photometry for F and G stars, mainly based on the work of Olsen. A number of problems in using this photometry and available calibrations have been described in Twarog et al. (2002) and Haywood (2002). Although several new calibrations have been published since then, we want to point out that problems still remain (see Haywood 2005). This is visible in Figure 3, which shows the metallicity for a number of stars of the Hyades cluster determined with different recent calibrations. The spectroscopic metallicity of the Hyades is bracketed within  $[+0.10, +0.15]$ , while all photometric determinations in Figure 3 underestimate this value by 0.1–0.3 dex. This is of course crucial, first because, as we show below, the metallicity distribution of disc stars is remarkably tight; and second because any systematic effect depending on colour directly impacts on the age-metallicity relation, since B-V is also an age sequence.

## 3. A GENERAL PICTURE OF THE METALLICITY DISTRIBUTION IN THE SOLAR NEIGHBOURHOOD

Figure 4 shows a general picture of the metallicity distribution as a function of B–V colour in the solar neighbourhood. Metallicity has been derived from Geneva photometry. The figure shows several interesting patterns, the

most conspicuous being the increasing range of metallicity towards cooler stars, resulting from the inclusion of older stars, and overlapping of several populations. In particular, one can see the rise of the old, metal rich population at  $B-V > 0.65$ , and the contribution of the thick disc and halo, with the progressive displacement of the turn-off towards the blue for metal poor stars.

### (1) A-type stars, Figure 5

Distinction by spectral type shows that the clump of stars at  $0.15 < B-V < 0.35$  is made of A-type stars. While this not surprising, it shows that the spectral type is an efficient discriminant of the patterns seen on the (B–V, [Fe/H]) distribution. A more detailed look at individual spectral types shows that within the A-type group, objects with  $[Fe/H] > +0.2$  are mostly Am stars. Below this limit, the proportion of Am stars decreases with metallicity, most of the other objects being recognised as either a variable star, multiple system, or luminosity class III object.

### (2) F-type stars, Figure 6

Spectral types are efficient to differentiate the metallicity behaviors of F stars vs. A stars, these two types forming 2 distinct groups in the (B–V, [Fe/H]) distribution. Most of the stars which behave like outlayers at  $[Fe/H] > 0.2$  dex and  $B-V < 0.45$  are metallic, peculiar F stars, or stars in double systems. Keeping in mind that the B–V sequence is an age sequence, we note that the bluest objects (at  $B-V < 0.30$ ), which are also the youngest (in the mean), have a small dispersion (0.1 dex observed, probably less intrinsic). The progressive enlargement of the metallicity distribution towards redder objects within the F stars group reflects the inclusion of older objects.

We note that these two facts are a strong indication, although not a direct proof, that the galactic disc follows an age-metallicity relation: the plot shows no star with medium-low metallicity content at  $B-V < 0.4$ , or young ages. This is in contradiction with the claim of a high dispersion at all ages.

### (3) G and K stars, Figure 7

G and K stars cover roughly the same metallicity interval. Their histogram is broadened by the presence of stars of all ages and different stellar populations. The dispersion in [Fe/H], which increases from 0.1 dex to 0.25 dex between  $B-V = 0.4$  and 0.65, increases to 0.3 dex at  $B-V > 0.7$ , due to the inclusion of old, metal rich, objects.

The different shapes of the histograms in metallicity for different spectral types are particularly conspicuous in Figure 7, and reveals with clarity that spectral types sample quite differently the stellar populations in the solar neighbourhood. The F stars histogram contains no old metal rich stars, and its upper limit is clearly that of the disc, at a metallicity that is more or less that of the Hyades cluster. It contains stars down to  $[Fe/H] < -0.5$ , but in much more limited extent than G stars. On the contrary, G and K stars sample all local populations, and their metallicity histogram extends to higher and lower limits, and is much broader than the F star distribution.

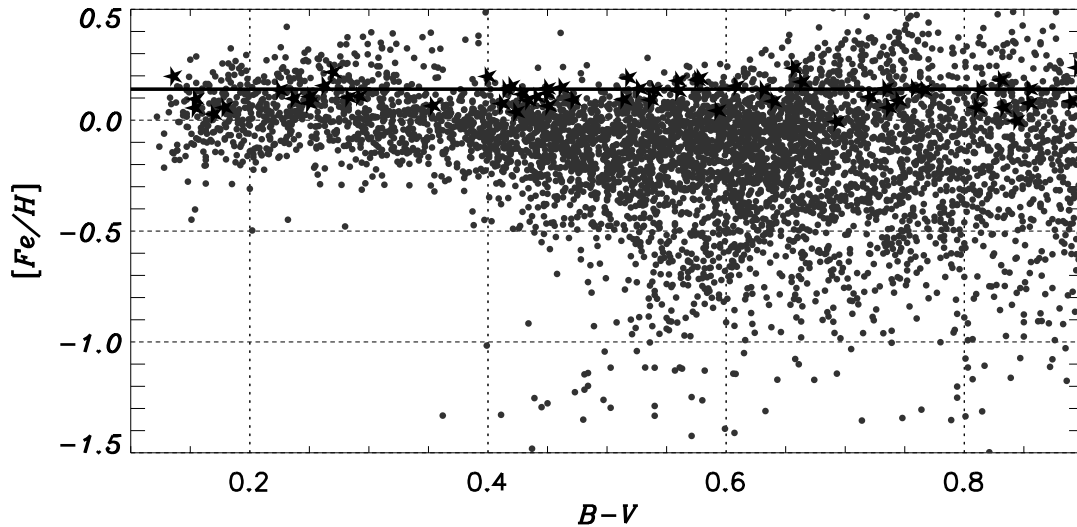


Figure 4. Metallicity distribution of stars in the solar vicinity. The metallicity is calculated using Geneva photometry. The star symbols around metallicity  $+0.14$  dex are Hyades stars with metallicity calculated using the same calibration (see Haywood 2005)

## 4. THE AGE-METALLICITY RELATION AND STAR FORMATION HISTORY

### 4.1. A Simple Test

In order to evaluate the effect of systematic and random errors on the determination of age trends, we apply the following simple procedure. We assume a model AMR or SFH, from which we generate a sample of points in the HR diagram, using a set of isochrones (Pols et al. 1998). We restrain our simulated sample to 5000 ‘stars’ with absolute magnitude  $2 < M_v < 5$ , in order to keep objects showing the largest evolutionary effects.

A systematic bias and random error is introduced on one or several of the atmospheric parameters  $M_v$ ,  $T_{\text{eff}}$ ,  $[\text{Fe}/\text{H}]$ , from which we try to recover the age using the isochrone fitting method (and the same set of isochrones). We can then compare the resulting ages with the initially assumed relations. The advantage of the method is that we test what can be expected from the data only, with no interference from the stellar models, keeping in mind that stellar models are a source of uncertainty that is difficult to evaluate, but can generate similar effects to those presented here, if the models are too hot, too cold, etc. Also, the test is a simplified one, and does not take into account effects such as unresolved binaries.

### 4.2. Present Achievements

The assumed AMR is presented on Figure 8a, composed of one monotonic increase of metallicity from  $-0.6$  dex 13 Gyrs ago to  $+0.11$  dex at the present time, with an intrinsic dispersion of 0.1 dex at all ages. A small clump of

stars with age 10 Gyrs and  $[\text{Fe}/\text{H}] = +0.1$  dex represents the metal rich population that is seen in Figure 4. Note that these parameters are chosen only for convenience, they have not been determined from data. We first apply our test with the uncertainties on the atmospheric parameters as evaluated in Section 2, that is 150 K and 0.15 dex in random errors, and  $-150$  K and  $-0.15$  dex systematics in effective temperature and metallicity, assuming these are representative of the present errors that are made on these parameters. The recovered AMR is seen in Figure 8b. It shows several interesting effects: a high dispersion at all ages, a large pattern at  $[\text{Fe}/\text{H}] = -0.2$  dex, 2 Gyrs, and, most important, the initial correlation between age and metallicity is lost. It must be noted that the first 2 characteristics (high dispersion at all ages and a large, spurious, clump of stars at 2–3 Gyrs) are common in recent determinations of the AMR based on Strömgren photometry, and that are affected by the biases mentioned in Section 2.

The pattern at  $[\text{Fe}/\text{H}] = -0.2$  dex, 2 Gyrs, is a direct consequence of the systematic bias in temperature and metallicity, and clearly shows that such biases can create spurious structures in the AMR. Note also that this is a simplified case: we have assumed that the bias is the same at all colours.

Figure 8c shows what can be recovered from the initial AMR, after having improved the determinations of atmospheric parameters. We assume that systematic biases in metallicity and effective temperatures have been corrected, that the random error on effective temperature are of the order of 50 K, a precision that can reasonably be achieved when using effective temperature indicators based on visual and near-infrared colour, such as V–I or V–K. On the other hand, it is unlikely that the uncertainty in metallicity as derived from photometry for

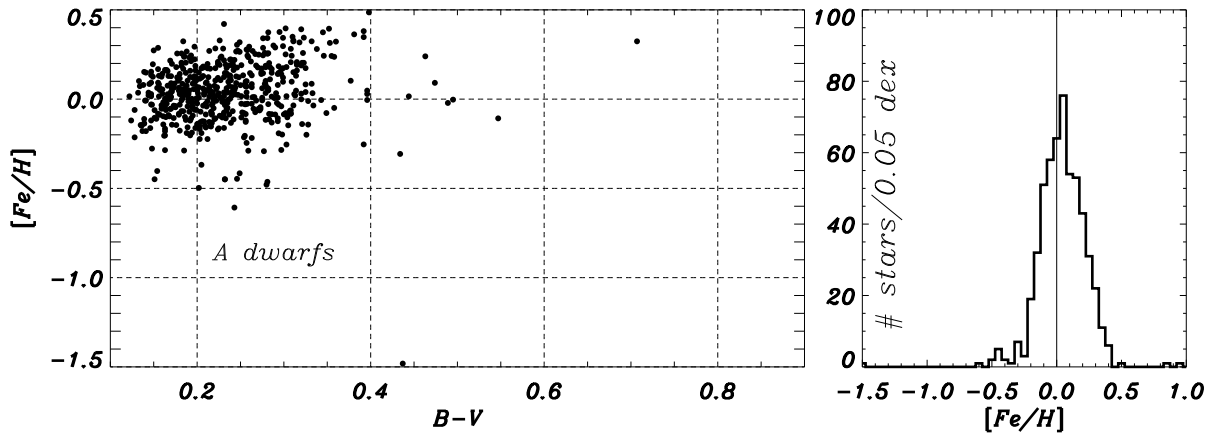


Figure 5. Metallicity distribution for A-type stars.

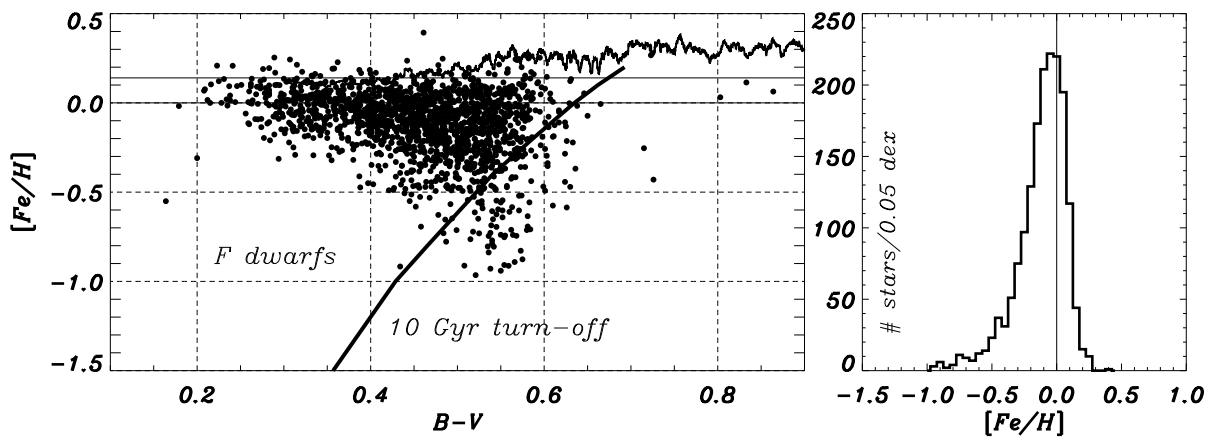


Figure 6. Metallicity distribution for F-type stars. The upper curve is the dispersion in  $[Fe/H]$  calculated as a function of  $B-V$  for 50 objects. The lower curve is the turn-off point at 10 Gyrs.

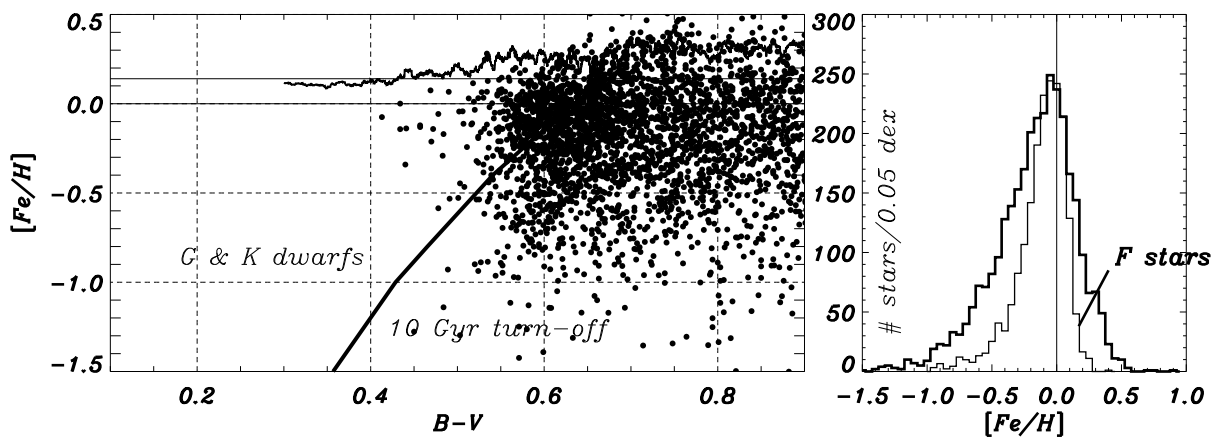


Figure 7. Metallicity distribution for G- and K-type stars. Legend same as Figure 6.

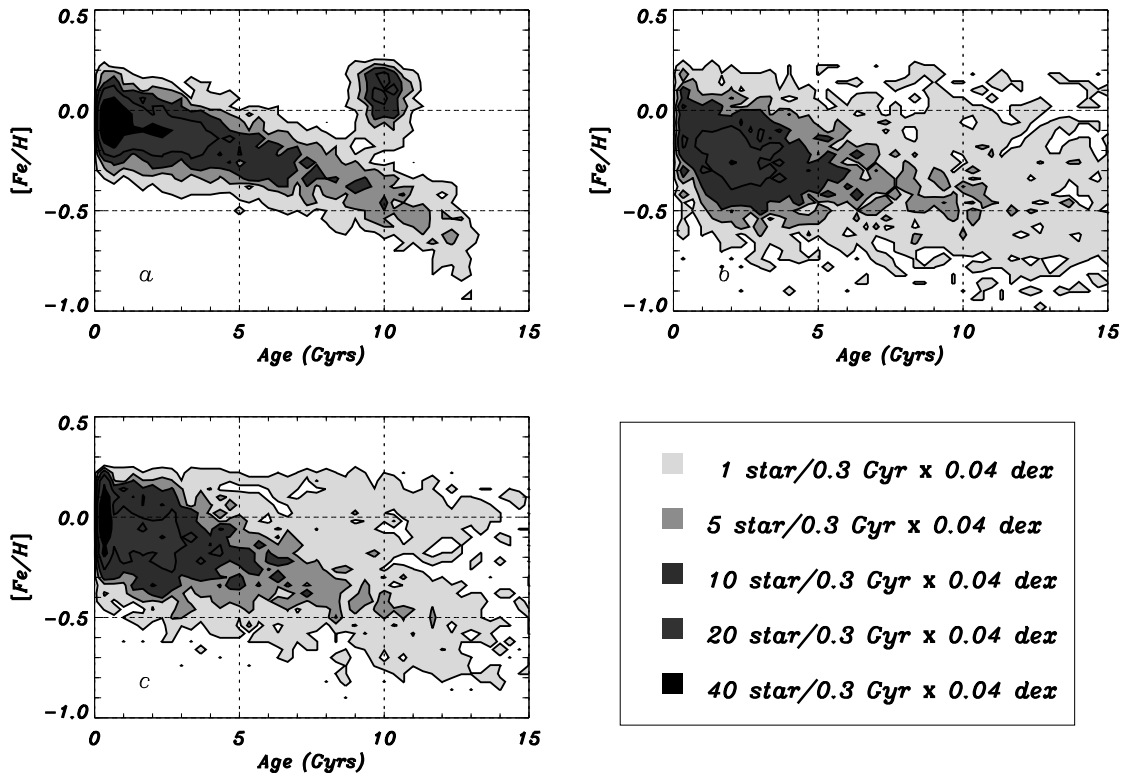


Figure 8. (a) The assumed age-metallicity distribution. (b) The age-metallicity recovered assuming systematic bias of  $-150$  K and  $-0.15$  dex, random errors of  $150$  K and  $0.15$  dex. (c) AMR recovered assuming no systematic bias, and  $50$  K and  $0.15$  dex random errors.

large sample of stars is going to improve in the next few years before Gaia. As expected, the spurious pattern at  $[\text{Fe}/\text{H}] = -0.2$  dex,  $2$  Gyrs has been removed because no systematic bias is introduced. A small trend in metallicity is detectable, although it is largely washed out by the still high dispersion in metallicity. The information about a separated population at  $10$  Gyrs and  $[\text{Fe}/\text{H}] = +0.1$  dex is lost, but could possibly be recovered using a more sophisticated analysis.

## 5. PROSPECTS WITH GAIA

According to the assessments of the Photometry Working Group, it is expected that the adopted photometric system could permit the determination of effective temperature to better than  $50$  K and metallicity to  $0.05$  dex, for F and G stars brighter than  $V = 18$ , in the case of no interstellar extinction. Given the improvement on the measurement of atmospheric parameters, and the expected impact on the calibration of stellar models over all the HR diagram, that implies much better conditions for measuring ages of stars over several kpc than is presently feasible with Hipparcos within  $100$ pc.

Figure 9a shows the AMR recovered assuming no bias in the atmospheric parameters,  $0.05$  dex random uncertainties in  $[\text{Fe}/\text{H}]$ ,  $50$  K in  $T_{\text{eff}}$ ,  $10\%$  relative accuracy in parallaxes. As can be seen, the trend of metallicity with age is almost entirely recovered, with a small dis-

persion, smearing part of the metal rich population. Figure 9b shows the result in the case where we restrict the selection to the best parallaxes with relative accuracy of  $1\%$ . In this case, most of the information can be visually recovered from the plot, although the old metal-rich population is still dispersed in age and metallicity. In the previous cases, we have assumed that the extinction plays no role, which is the case within a sphere of approximately  $75$  pc around the Sun (see Vergely et al. 2002). However, most of the photometric data in the Gaia Catalogue will be polluted to some extent by interstellar dust. The ability to correct for extinction and reddening using the photometric and spectroscopic data in Gaia is not entirely clear, however, it seems that in the case of moderate extinction ( $A_V < 1$  mag), the reddening could be corrected within  $0.03$ mag. That translate to approximately  $100$ – $150$  K in temperature on individual stars, which means a substantial loss of information.

Fig 10 shows results of the SFH recovered assuming  $50$  K uncertainty on effective temperature,  $0.05$  dex on metallicity and  $10\%$  relative accuracy on parallaxes. The plot shows the histograms of ages for the initial and recovered distributions. In the first case, with a slowly varying SFR, the general trend is correctly recovered, although peculiarities such as the peak of metal-rich stars at  $10$  Gyrs is not recovered from the initial data. In the second case, where the SFR is represented as a series of 3 prominent bursts at  $3$ ,  $5$  and  $7$  Gyrs, the information is lost and only a broad increase in the SFR between  $2$  and  $7$  Gyrs is detected.

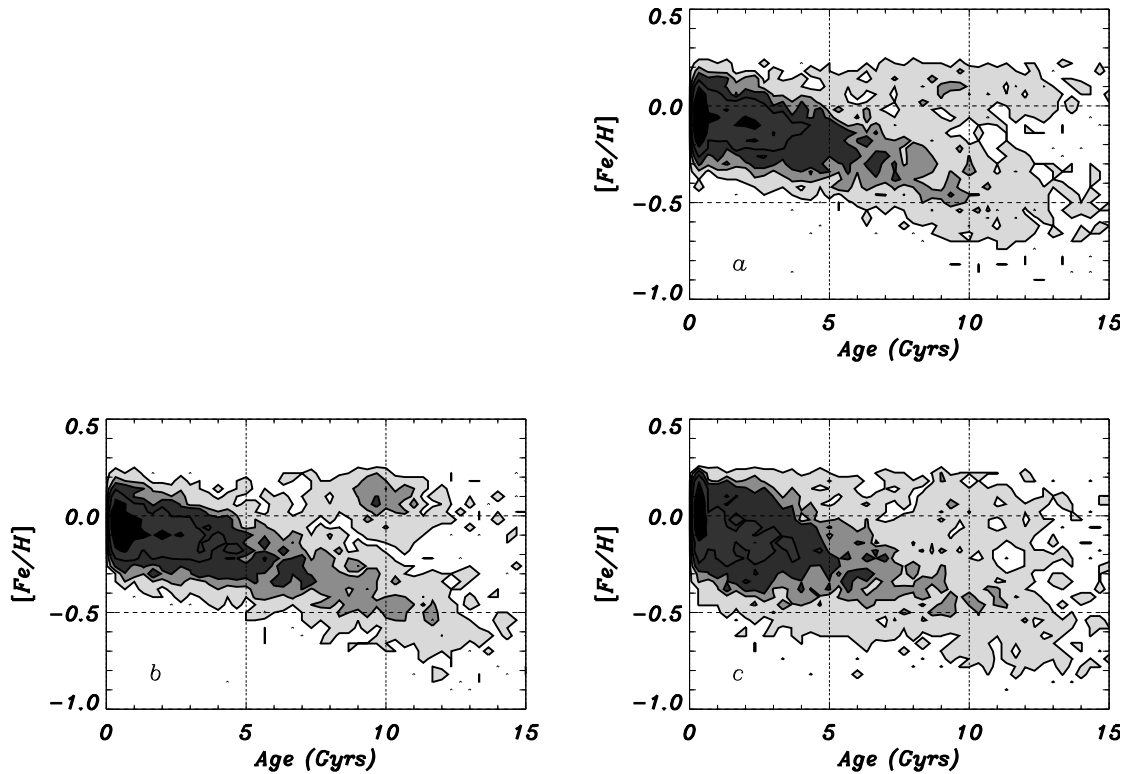


Figure 9. The AMR, assuming different uncertainties in the Gaia Catalogue. In (a), we assumed a typical uncertainty at  $V = 18$  or 0.05 dex and 50 K in  $[Fe/H]$  and  $T_{\text{eff}}$ , no extinction, 10% relative uncertainty in parallax. In (b), the same parameters except we assume 1% relative uncertainty in parallaxes. In (c), we assume 100K and 0.05 dex in  $T_{\text{eff}}$  and  $[Fe/H]$ , considering that this cases are representative of in cases of moderate extinction ( $A_v < 1$  mag).

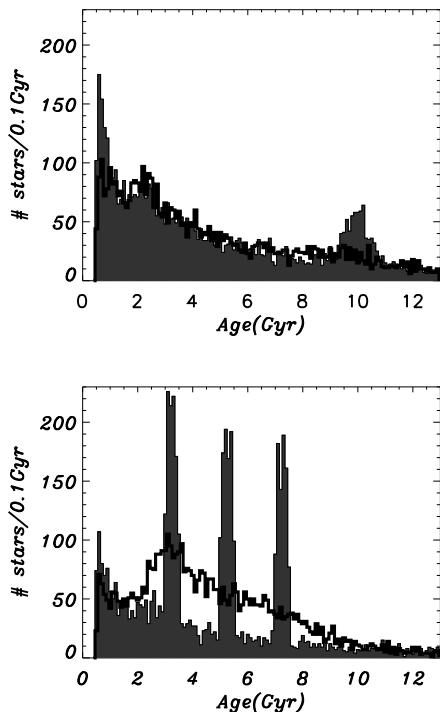


Figure 10. Initial (grey) and recovered (thick curve) Star Formation Histories, in case  $\sigma([Fe/H]) = 0.05$  dex  $\sigma(T_{\text{eff}}) = 50$  K and 10% uncertainty on parallax, for 2 different star formation histories.

## REFERENCES

- Barry, D.C., 1988, *Astrophys. J.*, 334, 436
- Bertelli, G., Nasi, E., 2001, *Astron. J.*, 121, 1013
- Edvardsson, B., Andersen, J., Gustafsson, B., et al., 1993, *Astronomy and Astrophysics Supplement Series*, 102, 603+
- ESA, 1997, *The Hipparcos and Tycho Catalogues*, ESA SP-1200
- Feltzing, S., Holmberg, J., Hurley, J.R., 2001, *Astron. Astrophys.*, 377, 911
- Gratton, R.G., Carretta, E., Castelli, F., 1996, *Astron. Astrophys.*, 314, 191
- Haywood, M., 2002, *Mon. Not. R. Astron. Soc.*, 337, 151
- Haywood, M., 2005, in preparation
- Hernandez, X., Valls-Gabaud, D., Gilmore, G., 2000, *Mon. Not. R. Astron. Soc.*, 316, 605
- Ibukiyama, A., Arimoto, N., 2002, *Astron. Astrophys.*, 394, 927
- King, I., 1971, *Publ. Astron. Soc. Pac.*, 83, 377
- Nordström, B., Mayor, M., Andersen, J., et al., 2004, *Astron. Astrophys.*, 418, 989
- Pols, O., Schroder, K.P., Hurley, J., Tout, C., Eggleton, P., 1998, *Mon. Not. R. Astron. Soc.*, 298, 525
- Pont, F., Eyer, L., 2004, *Mon. Not. R. Astron. Soc.*, 351, 487
- Powell, A., 1972, *Mon. Not. R. Astron. Soc.*, 155, 483

- Rocha-Pinto, H.J., Maciel, W.J., Scalo, J., Flynn, C., 2000a, *Astron. Astrophys.*, 358, 850
- Rocha-Pinto, H.J., Scalo, J., Maciel, W.J., Flynn, C., 2000b, *Astrophys. J., Lett.*, 531, L115
- Soderblom, D.R., Duncan, D.K., Johnson, D.R.H., 1991, *Astrophys. J.*, 375, 722
- Twarog, B.A., Anthony-Twarog, B.J., Tanner, D., 2002, *Astron. J.*, 123, 2715
- Vergely, J.L., Köppen, J., Egret, D., Bienaymé, O., 2002, *Astron. Astrophys.*, 390, 917